

Energetics and Electronic Properties of Interstitial Chlorine in CdTe

Walter Orellana,* Eduardo Menéndez-Proupin, and Mauricio A. Flores

The role of interstitial chlorine in the electronic properties of CdTe is addressed by density functional theory calculations including hybrid functionals and large unit cells. The stability and diffusion energy barriers of the impurity are analyzed as a function of the Fermi level position in the band gap. Chlorine is found to be stable in at least five interstitial sites with rather close formation energies, suggesting that they are all probable to be found. In *p*-type CdTe, the most stable sites are at the center of a Cd–Te bond and at a split-interstitial configuration, both acting as shallow donors. Whereas in *n*-type CdTe, it is found at the tetrahedral site surrounded by Cd hosts, acting as a shallow acceptor. We also find that chlorine can induce a deep acceptor level in the bandgap after binding with three Cd host atoms, which can explain the experimentally observed high resistivity in Cl-doped CdTe. The energy barriers for chlorine diffusion in both *p*-type and *n*-type CdTe are also discussed.

1. Introduction

Cadmium telluride (CdTe) is a II–VI semiconductor of considerable technological importance for a wide range applications such as photovoltaics, medical imaging, and high-energy astronomy.^[1–4] Due to its high atomic numbers and high mobility-lifetime product ($\mu\tau$), CdTe is a very attractive material for α - and γ -radiation detection offering many advantages over other semiconductors, such as silicon and germanium. Among photovoltaics, CdTe is one of the most promising materials due its near-optimum band gap of ≈ 1.5 eV, high absorption coefficient, and low manufacturing cost.^[5–8] In addition of good carrier transport properties, high-

performance radiation detectors also require high electrical resistivity for a low leakage current.^[9–12] The latter property may be achieved by controlled compensation between donors and acceptors,^[13] but it is very challenging in practice.^[14] In the case of CdTe, native defects, grain boundaries, and impurities may introduce electron or hole traps, decreasing the concentration and mobility of free carriers.

High resistivity CdTe can be prepared by the incorporation of group IV elements such as Ge or Sn.^[15–17] These impurities introduce deep energy levels in the bandgap, pinning the Fermi level near midgap and leading to a highly resistive material. Moreover, they act as deep donors that contribute to stabilize the compensation condition by transferring their electrons to uncompensated acceptors, commonly associated to Cd vacancies (V_{Cd}), which are

found to be abundant in CdTe.^[18] However, the main drawback of this procedure is that deep levels are also traps for electrons or holes and may act as effective recombination or lifetime killer centers, drastically decreasing the $\mu\tau$ product.^[19–21] Indeed, photoluminescence (PL) measurements of CdTe:Sn and CdTe:Ge show an intense energy peak near midgap, indicating a radiative recombination activity.^[22–24]


Chlorine doping is another well-established route to obtain high resistivity in CdTe.^[13,14,25–27] Studies on single-crystal CdTe:Cl indicate a hole trap near midgap.^[28–30] However, the compensation mechanism responsible for the observed semi-insulating condition is still debated and remains as an open issue. An explanation proposed by Biswas et al.^[13] suggests that the observed high resistivity in CdTe:Cl is due to compensation between shallow donors (Cl_{Te}) and shallow acceptors (V_{Cd}). However, it was argued by Krasikov et al.^[14] that shallow defect levels alone, although theoretically possible, are unlikely to cause high resistivity.

Regarding the stable sites and diffusion pathways of Cl interstitials in CdTe (Cl_i), there are also controversial results. First-principles calculations including hybrid functionals have reported that Cl_i is stable in the middle between two neighboring Cd atoms in neutral charge state and at the tetrahedral site surrounded by Cd atoms in the single negative charge state, acting as a shallow donor and shallow acceptor, respectively.^[31–34] In addition, diffusion barriers for neutral and single negative Cl are estimated in 0.3 and 0.9 eV, respectively.^[33] Other works have reported that Cl in positive charge states is found stable in the bond center site, in the middle of a Cd–Te bond,^[26] where diffusion energy barriers are estimated around 1.2 eV. On the other hand, experimental results have

Prof. W. Orellana
Departamento de Ciencias Físicas
Universidad Andrés Bello
Sazié 2212, Santiago 8370136, Chile
E-mail: worellana@unab.cl

Prof. E. Menéndez-Proupin
Facultad de Ciencias
Departamento de Física
Universidad de Chile
Las Palmeras 3425, Ñuñoa 7800003, Chile

M. A. Flores
Facultad de Ingeniería y Tecnología
Universidad San Sebastián
Bellavista 7, Santiago 8420524, Chile

 The ORCID identification number(s) for the author(s) of this article can be found under <https://doi.org/10.1002/pssb.201800219>.

DOI: 10.1002/pssb.201800219

established activation energies between 0.63 and 1.32 eV measured in the temperature range of 200–700 °C.^[35]

In this work, we study the stability, electronic properties and minimum energy pathway of interstitial Cl in CdTe by first-principles calculations including hybrid functionals. In order to minimize size effects, large supercells with 250 atoms were used. We find that chlorine is stable in at least five interstitial sites with close formation energies, showing different electronic properties. It can act as shallow acceptor, shallow donor, and also as a deep-level recombination center, depending on the site into which it is introduced. The latter case would be responsible for the high resistivity observed in Cl-doped CdTe. Minimum-energy path and formation energy calculations suggest that Cl_i diffuses through bond-center sites in *p*-type CdTe preferentially in single positive and neutral charge states, with activation energies of 0.50 eV. Whereas, in *n*-type CdTe, Cl_i diffuses through tetrahedral interstitial sites, preferentially in neutral charge state, with activation energies of 0.65 eV.

2. Theoretical Approach

Our calculations were performed in the framework of density-functional theory (DFT), using the Vienna Ab Initio Simulation Package.^[36] Hybrid functional was used to describe the exchange correlation term as proposed by Heyd, Scuseria and Ernzerhof (HSE06),^[37] in which 25% of the Hartee-Fock exchange is mixed with 75% of the Perdew-Burke-Ernzerhof semi-local functional (GGA-PBE). The core-valence interactions are included by using the projected augmented wave approach.^[38] Equilibrium geometries and formation energies were obtained with 250-atom supercells. The band structures were obtained with smaller 128-atom supercells due to the great computational cost that these calculations require. For both supercells, the self-consistent calculations were performed using the Γ point for the Brillouin zone sampling. Convergence tests for neutral Cl_i in CdTe using the 128-atom supercell and a $2 \times 2 \times 2$ k-point mesh were performed. Our results show that the difference in total energy between both k-point samples is less than 0.02 eV atom⁻¹, while the band structures show negligible variations. Wave functions were expanded in a plane-wave basis set with a cutoff energy of 285 eV. With these parameters, the bandgap and lattice constant of CdTe are calculated to be of 1.44 eV and 6.566 Å, respectively. Increasing the cutoff energy up to 400 eV shows variations less than 1% in the lattice constant and negligible variation in the bandgap. The systems were fully relaxed until the residual force on each atomic component was less than 0.025 eV Å⁻¹. The minimum energy path for the chlorine diffusion in CdTe in different charge states were calculated using the climbing-image nudged elastic band (NEB) methods.^[39] As the diffusion barriers depend on different atomic configurations involved in the process of diffusion,^[40] with the NEB method we have obtained the lowest bound for the diffusion barrier. The calculations were performed with a 128-atom supercell with all atoms left free to relax. First, we use the GGA-PBE functional to obtain the minimum-energy geometries of ten intermediate images and then we re-evaluate the single-point energy of each image using the HSE06 functional.

The formation energies and thermodynamic transition-energy levels of interstitial chlorine in CdTe are calculated

according to the well-established scheme discussed in ref. [41]. For interstitial chlorine in charge state q (Cl_i^{*q*}), the formation energy (ΔH_f) as a function of the Fermi level (E_F) is obtained as

$$\Delta H_f(\text{Cl}_i^q) = E(\text{Cd}_n\text{Te}_n\text{Cl}; q) - E(\text{Cd}_n\text{Te}_n) - \mu_{\text{Cl}} + q(E_{\text{VBM}} + E_F) \quad (1)$$

where $E(\text{Cd}_n\text{Te}_n)$ is the total energy of a supercell containing n primitive cells of CdTe. $E(\text{Cd}_n\text{Te}_n\text{Cl}; q)$ is the energy the same supercell with one Cl and q electrons removed. Moreover, μ_{Cl} is the chemical potentials of Cl, and E_{VBM} is the energy of the valence band maximum (VBM).

The chemical potentials of the atomic species are defined as

$$\mu_X = E_X + \Delta\mu_X, \text{ with } X = \text{Cd, Te, or Cl} \quad (2)$$

where E_X is the energy per atom of species X in a reference state, which are the solid bulk phases of Cd and Te, and the gas phase Cl₂.

In addition, thermodynamics imposes some restrictions to the chemical potentials,

$$\Delta\mu_{\text{Cd}} \leq 0, \Delta\mu_{\text{Te}} \leq 0, \Delta\mu_{\text{Cl}} \leq 0 \quad (3)$$

$$\Delta\mu_{\text{Cd}} + \Delta\mu_{\text{Te}} = \Delta H(\text{CdTe}) = -1.17 \text{ eV} \quad (4)$$

$$2\Delta\mu_{\text{Cl}} + \Delta\mu_{\text{Cd}} \leq \Delta H(\text{CdCl}_2) = -3.59 \text{ eV} \quad (5)$$

Inequalities (3) represent the conditions for pure compounds not to segregate. $\Delta\mu_{\text{Cd}} = 0$ and $\Delta\mu_{\text{Te}} = 0$ are the so-called Cd-rich and Te-rich conditions, respectively. Equation (4) accounts for the presence of CdTe in equilibrium, while inequality (5) is the condition for CdCl₂ phase not to segregate. $\Delta H(\text{CdTe})$ and $\Delta H(\text{CdCl}_2)$ are the formation heats, with the numerical values obtained from HSE calculations. Other inequalities similar to (5) can be set to account for no formation of other compounds like TeCl₄, and Te₃Cl₂, but in practice (5) sets the maximum possible value for $\Delta\mu_{\text{Cl}}$ in equilibrium with CdTe. $E(\text{Cd}_n\text{Te}_n\text{Cl}; q)$ in Equation (1) includes size corrections for image charge and potential alignment as defined in refs. [42,43]. Thus, according to ref. [43], no correction for band-filling is needed, as we use only the Γ point to sample the Brillouin zone.

3. Results and Discussion

As an isolated interstitial impurity in CdTe, chlorine (Cl_i) can occupy a number of different lattice sites. To find their stable positions we first locate the Cl atom at six points of high symmetry in the lattice, namely at the two tetrahedral sites nearest neighbor to Cd and Te atoms (T_1 and T_2 , respectively); at the center of the Cd–Te bond (BC); at the hexagonal site (H), and at the middle of the line joining two nearest-neighbor Te atoms and Cd atoms (C_1 and C_2 , respectively). After relaxation, Cl_i initially at C_2 and H sites moves toward the T_1 site; Cl_i at the C_1 initial site moves toward a split-interstitial configuration, that is, a Cl–Cd dimer occupying a Cd site surrounded by Te atoms

(hereafter referred simply as C_1). Finally, Cl_i at T_1 , T_2 , and BC initial sites remains approximately close to their original positions, inducing some distortions the neighboring atoms.

Figure 1 shows equilibrium geometries and band structures of Cl_i at C_1 and BC sites. At the C_1 site, chlorine is found threefold coordinated binding with one Cd atom and two Te atoms with Cl–Cd and Cl–Te bond distances of 2.57 and 2.71 Å, respectively. At the BC site chlorine locates in the center of a Cd–Te bond with Cd–Cl and Cl–Te bond distances of 2.69 and 2.39 Å, respectively, and Cd–Cl–Te angle of 134° . The band structures show that Cl_i at C_1 and BC sites acts as a single donor, as the Fermi level locates at the bottom of the conduction band, where impurity level (c_2) is found resonant in the conduction band. The charge density isosurfaces of the c_2 level indicate that the impurity state has an antibonding character.

Figure 2 shows equilibrium geometries and band structures of Cl_i at T_1 and T_2 sites. At the T_1 site, chlorine locates 2.7 Å from the Cd atom along the $\langle 111 \rangle$ direction, almost without disturbing the neighboring atoms. The distance between Cl and the other Cd atoms is found of 2.90 Å. Figure 2(a) shows the band structure, which indicate a shallow acceptor character as the Fermi level locates at the top of the conduction band. The charge density isosurfaces of the half-occupied ν_1 level shows a delocalization, characterizing the acceptor state. At the T_2 site,

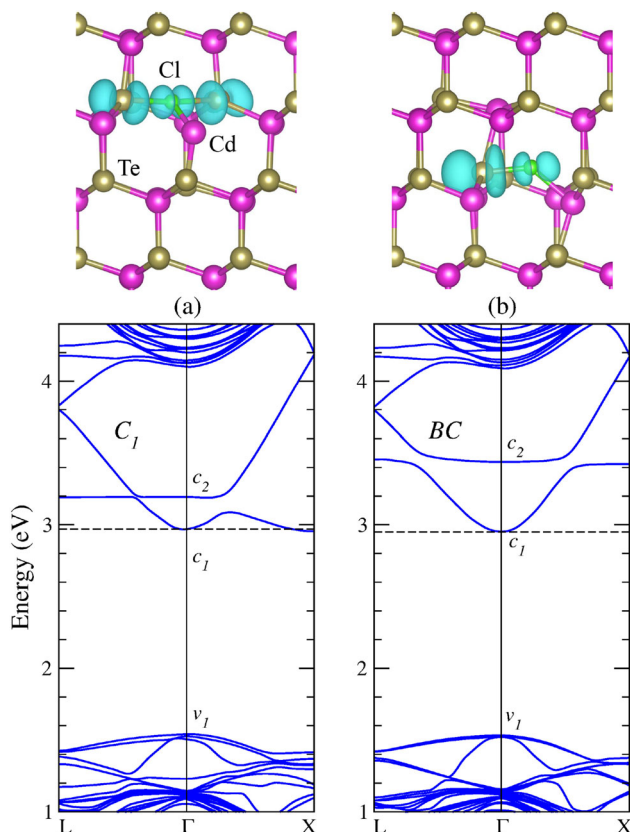


Figure 1. Equilibrium geometry and band structure neutral Cl in CdTe, (a) at the C_1 site, and (b) at a BC site. The dashed line indicates the Fermi energy. Charge density isosurfaces of the impurity level (c_2) of C_1 and BC are plotted for $\rho = 0.005 \text{ eÅ}^{-3}$.

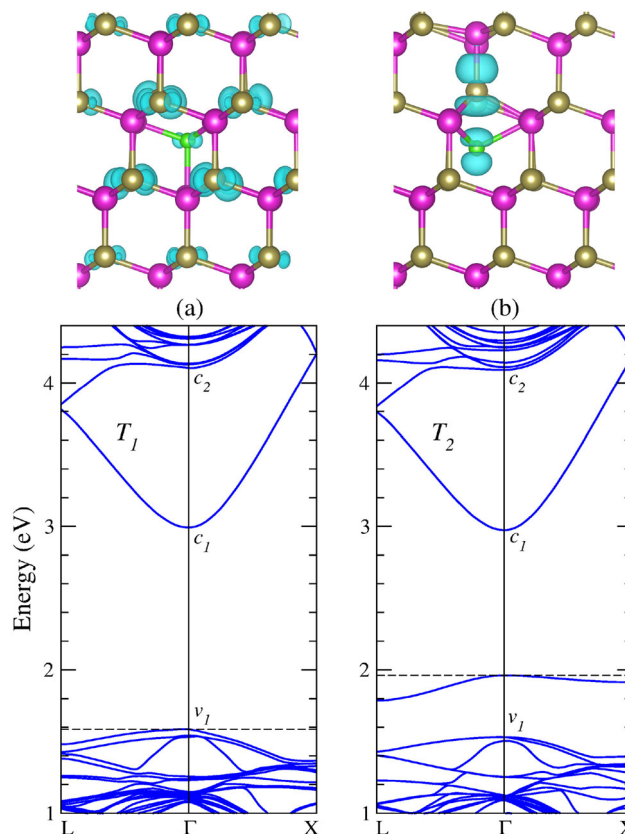


Figure 2. Equilibrium geometry and band structure of neutral Cl in CdTe, (a) at the T_1 site, and (b) at the T_2 site. The dashed line indicates the Fermi energy. Charge density isosurfaces of the ν_1 level of T_1 and the gap level of T_2 are plotted for $\rho = 0.0008$ and 0.005 eÅ^{-3} , respectively.

chlorine moves from the initial tetrahedral site surrounded by Te atoms, about 0.4 Å along the $\langle 111 \rangle$ direction, binding with the three Cd nearest neighbors. The formation of these bonds induces a strong distortion in the neighboring Te–Cd bond, which is displaced from its lattice position by about 0.53 Å along the $\langle 111 \rangle$ direction. The bond distances between Cl and the three Cd atoms is found of 2.97 Å. Figure 2(b) shows the band structure of Cl_i at the T_2 site in the equilibrium geometry. We find a single occupied defect level in the bandgap not previously reported. The charge density isosurfaces of this level indicate localization as well as an antibonding character, which characterize the defect level. Therefore, at the T_2 site, chlorine acts as a deep acceptor, which can be the origin of the high resistivity observed in Cl-doped CdTe.

We also study another split-interstitial configuration for chlorine previously reported by Yang et al.,^[33] hereafter referred as *Spl*. According to ref. [33], positively charged Cl can lower its energy by forming a Cl–Te bond, occupying the Te atomic site. Our results show that the *Spl* site is stable with almost the same energy than our BC site, however, it shows a slightly different geometry. We find that neutral and positively charged Cl do not bind with the Te atom. Instead it binds with its three Cd nearest neighbors, while the Te atom removed from its lattice sites, binds with Te and Cd nearest neighbors. The calculations of

ref. [33] were performed including the HSE06 functional within a 64-atom supercell, therefore the discrepancy with our results can be attributed to size effects. In addition, Cl_i at the Spl configuration acts a shallow donor similar to Cl_i at the BC site.

The stability of the Cl_i impurity at different equilibrium sites is analyzed by comparing their formation energies as a function of the Fermi level, according to Equation (1). Our results are shown in **Figure 3**. We observe that chlorine at the stable sites under study have close formation energies, within an energy range of about 1 eV, suggesting that they are equally probable to be found. According to Figure 3, Cl_i at BC and Spl sites show the lower formation energies in p -type CdTe, while Cl_i at the T_1 site shows the lowest formation energy in n -type CdTe. Therefore, they are likely to be found at higher concentrations inducing shallow energy levels of donor and acceptor types, respectively. In absence of native defects like V_{Cd} , the lower formation energies of donor-acceptor systems suggest a self-compensation between Cl_i^{1+} (BC) and Cl_i^{1-} (T_1), and between Cl_i^{1+} (Spl) and Cl_i^{1-} (T_1), with $\epsilon(+/-)$ transition states at $\text{VBM} + 0.65$ and $\text{VBM} + 0.75$ eV, respectively. The self-compensation is understood as the response of an active impurity system to the introduction of another active impurity, which tend to compensate their electrical activity through the formation of opposite charged defects.^[44,14] Self-compensation by the same impurity has been also suggested in P-doped CdTe.^[45]

Previous DFT-HSE06 calculations have analyzed the role of Cl_i -related shallow donors and shallow acceptors in the self-compensation property.^[26] The authors report a $\epsilon(+/-)$ transition state at $\text{VBM} + 0.8$ eV associated to Cl_i in CdTe, in close agreement with our results. However, they proved that donor-acceptor self-compensation is not a sufficient condition to explain the experimentally observed high resistivity in Cl-doped CdTe,^[28–30] proposing the deep-acceptor complex $\text{Cl}_{\text{Te}}-\text{Cl}_{\text{Cd}}$ as the possible reason for that. According to our results, Cl_i at the T_2

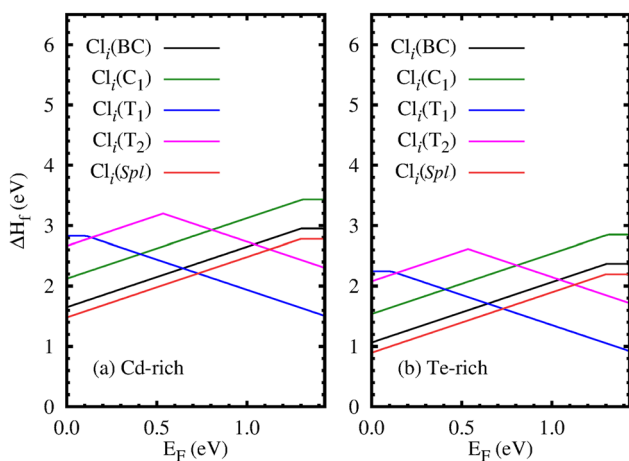


Figure 3. Formation energy (ΔH_f) as a function of the Fermi level (E_F) in the bandgap for interstitial chlorine in CdTe in their different equilibrium geometries performed within a 250-atom supercell: (a) for Cd-rich conditions, and (b) for Te-rich conditions. The slopes of the formation energy indicate the charge states of the impurity (+1, 0, -1), while changes in its slopes indicates defect transition states.

site induces a strong lattice distortion, leading to a negative- U behavior where the neutral charge state is never stable. The $\epsilon(+/-)$ transition state, as obtained from Figure 3, is found at $\text{VBM} + 0.55$ eV, indicating that interstitial chlorine can introduce a deep level in the bandgap. We believe that this deep acceptor can be responsible for the Fermi level pinning that could explain the high resistivity in Cl-doped CdTe.

We now turn to examine the minimum-energy path of positive, neutral, and negative chlorine diffusing between two neighboring T_1 sites (as it would happen in n -type CdTe) and between BC sites (as it would happen in p -type CdTe), using the NEB method.^[39] **Figure 4** shows the minimum-energy path for Cl_i diffusing between T_1 sites for negative, neutral, and positive charge states, as obtained with GGA-PBE and HSE06 functionals. We include both calculations to stress the difference between XC functionals. We observe that HSE06 functional strengthened the interaction of Cl_i with the host atoms by increasing the steric repulsion. For Cl_i^{1+} we observe that the T_1 site is a local minimum and the intermediate geometry, which correspond to the C_1 sites previously found, is the global minimum. The energy barrier is found to be of

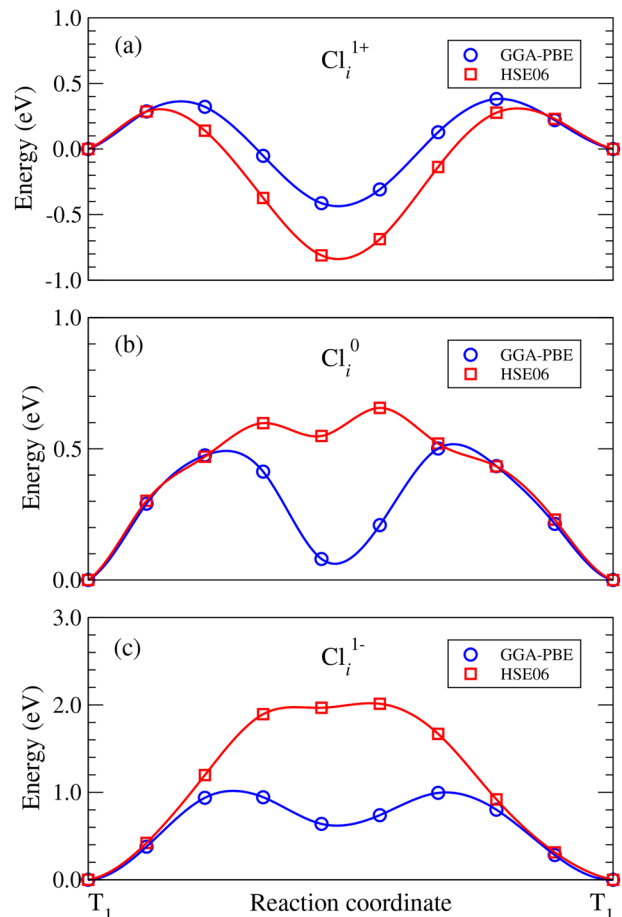


Figure 4. Minimum energy path for the chlorine diffusion between neighboring T_1 sites in n -type CdTe as calculated with GGA-PBE and HSE06 functionals in (a) positive, (b) neutral, and (c) negative charge state.

1.15 eV. The initial, intermediate and final geometries of the minimum-energy path are shown in **Figure 5**. For Cl_i^0 and Cl_i^{1-} the intermediate geometry is higher in energy than the T_1 site, showing barriers of 0.65 and 2.15 eV, respectively. According to the formation energies shown in Figure 3, chlorine is most stable at T_1 sites for n -type CdTe. Therefore, in this condition, it would diffuse preferentially in neutral charge state with an activation energy of 0.65 eV. Previous calculations performed with the local functional (LDA) have reported a global minimum for neutral Cl_i in CdTe at the T_1 site and minimum-energy path between neighboring T_1 sites showing a plateau with a maximum energy of 0.68 eV.^[46] It is interesting to note that this LDA result differs from those of GGA, while approaching to the HSE06 one, as shown in Figure 4. We believe that the coincidence between LDA and HSE06 results is fortuitous and might be attributed to a cancelation error.

For p -type CdTe, formation energy calculations indicate that BC is one of the most stable sites for chlorine. Thus, we calculate the minimum-energy path for positive, neutral, and negative Cl_i diffusing through neighboring BC sites in CdTe. Our results are shown in **Figure 6**. We find that Cl_i would diffuse in positive and neutral charge states with almost the same activation energy of 0.49 and 0.52 eV, respectively, whereas in negative charge state the energy barrier is much more larger, of about 2.5 eV. The initial, intermediate and final geometries of the minimum-energy path are shown in **Figure 7**. Therefore, in p -type CdTe, chlorine would diffuse preferentially in neutral or positive charge states through BC sites with an activation energy of about 0.5 eV. In ref. [26] is suggested that the Cl_i^+ diffusion through the BC sites evolves through two steps: 1) by breaking $\text{Cl}-\text{Cd}$ bond and rotating around Te atom with an energy barrier of about 1.25 eV; and 2) by breaking $\text{Cl}-\text{Te}$ bond and rotating around Cd atom with an energy barrier of about 0.55 eV. Although our minimum energy path agree well with the step (1), we found lower activation energy for this diffusion path.

Figure 7(b) shows the atomic geometry for the energy maximum in the reaction coordinate of neutral and positively charged chlorine diffusing through BC sites. Here the Cl atom is in the middle of two nearest-neighbors Cd atoms close to a Te atom. However, previous GGA calculations,^[31] report that this geometry would be stable, being only 2 meV higher in energy

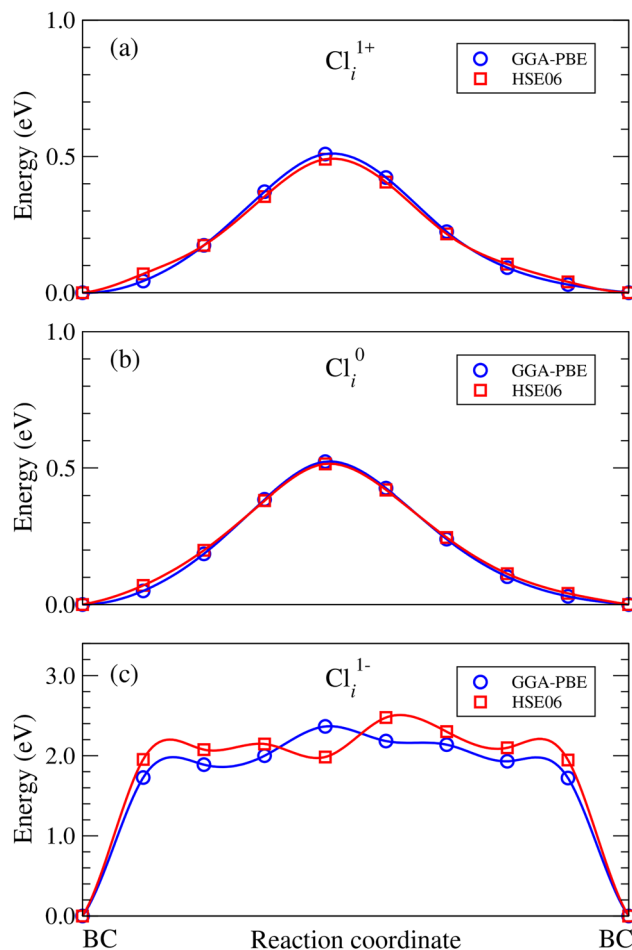


Figure 6. Minimum energy path for the chlorine diffusion between neighboring BC sites in p -type CdTe as calculated with GGA-PBE and HSE06 functionals in (a) positive, (b) neutral, and (c) negative charge state.

than the T_1 site. In the present work, the stable site reported in ref. [31] is not found. According to our results, when neutral Cl is located between two neighboring Cd atoms, it moves to the tetrahedral site T_1 , lowering its energy by 0.48 eV. We believe that the discrepancy may be originated in the semilocal GGA-PBE

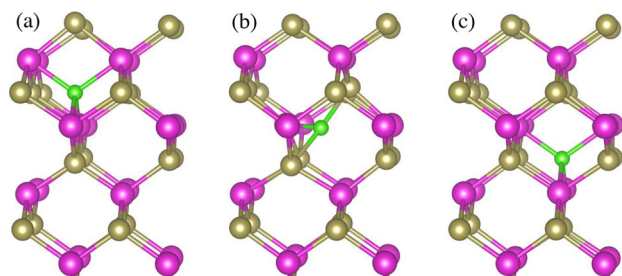


Figure 5. Atomic structure of Cl_i at neighboring T_1 sites (a) and (c), and at the intermediate geometry between T_1 sites in the minimum-energy path (b), which in this case corresponds to the stable C_1 site previously found (see Figure 1a).

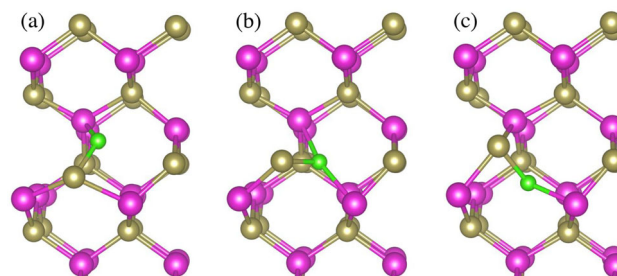


Figure 7. Atomic structure of Cl_i at neighboring BC sites (a) and (c), and at the intermediate geometry between BC sites in the minimum-energy path (b).

functional used in ref. [31]. In addition, concerning the exchange-correlation functional, we note that GGA-PBE and HSE06 results show quite close minimum-energy paths when chlorine strongly interacts with the host atoms through *BC* sites (Figure 6), contrasting with those found for the diffusion through T_1 sites (Figure 4), where the interaction with the host atoms is much weaker. This opens some doubt about the effectiveness of semilocal functionals to describe diffusion energy barriers.

4. Summary

In summary, we investigate the chlorine impurity in CdTe using DFT calculations including the hybrid HSE06 functional and large supercells, containing up to 250 atoms. For interstitial chlorine we find five stable sites with rather close formation energies, suggesting that they are all probable to be found in the CdTe lattice. The most stable sites are the bond center (*BC*) and the split-interstitial (*Spl*) in *p*-type CdTe, and the tetrahedral site surrounded by host Cd atoms (T_1) in *n*-type CdTe. Therefore, they are likely to be found at higher concentrations inducing shallow energy levels of donor and acceptor types, respectively. In addition, Cl_i at the tetrahedral site surrounded by host Te atoms (T_2) exhibits a strong lattice distortion after the formation of Cl-Cd bonds, that induces a deep level in the bandgap with transition state of $\epsilon(+/-) = 0.55$ eV. In addition, our results suggest donor-acceptor self-compensation mechanisms, that may lead to the Fermi-level pinning near midgap, can be associated solely to Cl interstitials. Models assuming self-compensation in heavily Cl-doped CdTe crystals support our finding.^[47] However, recent calculations indicate that donor-acceptor self-compensation cannot explain the experimentally observed high resistivity in Cl-doped CdTe.^[26] We propose that Cl_i at the T_2 site, a deep acceptor impurity, would be the origin of the high resistivity observed in Cl-doped CdTe. Finally, we study the chlorine diffusion in CdTe considering the position of the Fermi level. Our results suggest that chlorine diffuses in *p*-type CdTe preferentially in single positive and neutral charge states through the bond-center *BC* site with an activation energy of about 0.5 eV, whereas in *n*-type CdTe, it would diffuse preferentially in neutral charge state through tetrahedral interstitial sites surrounded by Cd hosts (T_1), with an energy barrier of 0.65 eV. Our results are in close agreement with available experimental data that report activation energies for chlorine diffusion between 0.63 and 1.32 eV measured in the temperature range of 200–700 °C.^[35]

Acknowledgements

We acknowledge support from Chilean funding agency FONDECYT under Grants No. 1170480 (W.O.) and 1171807 (E.M-P.). Powered@NLHPC: This research was partially supported by the supercomputing infrastructure of the NLHPC (ECM-02).

Conflict of Interest

The authors declare no conflict of interest.

Keywords

cadmium telluride, chlorine impurity, computational physics, density functional theory, diffusion energy, formation energy

Received: May 14, 2018
Revised: September 14, 2018
Published online: October 9, 2018

- [1] H. B. Barber, *Nucl. Instrum. Methods Phys. Res. A* **1999**, 436, 102.
- [2] L. Verger, M. Boitel, M. Gentet, R. Hamelin, C. Mestais, F. Mongellaz, J. Rustique, G. Sanchez, *Nucl. Instrum. Methods Phys. Res. A* **2001**, 458, 297.
- [3] C. Scheiber, G. C. Giakos, *Nucl. Instrum. Methods Phys. Res. A* **2001**, 458, 12.
- [4] M. Fiederle, V. Babentsov, J. Franc, A. Fauler, J.-P. Konrath, *Cryst. Res. Technol.* **2003**, 38, 588.
- [5] A. Morales-Acevedo, *Sol. Energy Mater. Sol. Cells* **2006**, 90, 2213.
- [6] C. S. Ferekides, U. Balasubramanian, R. Mamazza, V. Viswanathan, H. Zhao, D. L. Morel, *Sol. Energy* **2004**, 77, 823.
- [7] M. Gloeckler, I. Sankin, Z. Zhao, *IEEE J. Photovolt.* **2013**, 3, 1389.
- [8] K. Shen, Q. Li, D. Wang, R. Yang, Y. Deng, M.-J. Jeng, D. Wang, *Sol. Energy Mater. Sol. Cells* **2016**, 144, 472.
- [9] C. Scheiber, *Nucl. Instrum. Methods Phys. Res. A* **1996**, 380, 385.
- [10] M. Fiederle, C. Eiche, M. Salk, R. Schwarz, K. Benz, W. Stadler, D. Hofmann, B. Meyer, *J. Appl. Phys.* **1998**, 84, 6689.
- [11] S. Del Sordo, L. Abbene, E. Caroli, A. M. Mancini, A. Zappettini, P. Ubertini, *Sensors* **2009**, 9, 3491.
- [12] V. Lordi Point, *J. Cryst. Growth* **2013**, 379, 84.
- [13] K. Biswas, M. H. Du, *New J. Phys.* **2012**, 14, 063020.
- [14] D. Krasikov, A. Knizhnik, B. Potapkin, T. Sommerer, *Semicond. Sci. Technol.* **2013**, 28, 125019.
- [15] O. Panchuk, A. Savitskiy, P. Fochuk, Y. Nykonyuk, O. Parfenyuk, L. Shcherbak, M. Ilashchuk, L. Yatsunyk, P. Feychuk, *J. Cryst. Growth* **1999**, 197, 607.
- [16] A. V. Savitsky, *Opt. Mater.* **1991**, 38, 1349.
- [17] J. E. Jaffe, *J. Appl. Phys.* **2006**, 99, 033704.
- [18] A. Shepidchenko, B. Sanyal, M. Klintonberg, S. Mirbt, *Sci. Rep.* **2015**, 5, 14509.
- [19] M. Hage-Ali, P. Siffert, *Nucl. Instrum. Methods Phys. Res. A* **1992**, 322, 313.
- [20] M. Fiederle, D. Ebling, C. Eiche, D. Hofmann, M. Salk, W. Stadler, K. Benz, B. Meyer, *J. Cryst. Growth* **1994**, 138, 529.
- [21] M. A. Flores, E. Menéndez-Proupin, W. Orellana, J. L. Peña, *J. Phys. D: Appl. Phys.* **2016**, 50, 035501.
- [22] U. Pal, P. Fernández, J. Piqueras, N. V. Sochinskii, E. Diéguez, *J. Appl. Phys.* **1995**, 78, 1992.
- [23] J. Franc, M. Fiederle, V. Babentsov, A. Fauler, K. W. Benz, R. James, *J. Electron. Mater.* **2003**, 32, 772.
- [24] J. Franc, P. Hldek, E. Belas, J. Kubát, H. Elhadidy, R. Fesh, *Nucl. Instrum. Methods Phys. Res. A* **2008**, 591, 196.
- [25] C. Eiche, D. Maier, D. Sinerius, J. Weese, K. Benz, J. Honerkamp, *J. Appl. Phys.* **1993**, 74, 6667.
- [26] D. Krasikov, A. Knizhnik, B. Potapkin, T. Sommerer, *MRS Proc.* **2014**, 1638, 1.
- [27] J. Pousset, I. Farella, S. Gambino, A. Cola, *J. Appl. Phys.* **2016**, 119, 105701.
- [28] S. A. Ringel, A. W. Smith, M. H. MacDougal, A. Rohargi, *J. Appl. Phys.* **1991**, 70, 881.
- [29] A. Castaldini, A. Cavallini, B. Fraboni, P. Fernandez, J. Piqueras, *Phys. Rev. B* **1997**, 56, 14897.
- [30] A. Castaldini, A. Cavallini, B. Fraboni, P. Fernandez, J. Piqueras, *J. Appl. Phys.* **1998**, 83, 2121.

- [31] J. Ma, J. Yang, S. H. Wei, J. L. F. Da, *Phys. Rev. B* **2014**, *90*, 155208.
- [32] J. H. Yang, J. S. Park, J. Kang, S. H. Wei, *Phys. Rev. B* **2015**, *91*, 075202.
- [33] J. H. Yang, W. J. Yin, J. S. Park, W. Metzger, S. H. Wei, *J. Appl. Phys.* **2016**, *119*, 045104.
- [34] J. H. Yang, W. J. Yin, J. S. Park, J. Ma, S. H. Wei, *Semicond. Sci. Technol.* **2016**, *31*, 083002.
- [35] E. D. Jones, J. Malzbender, J. B. Mullins, N. Shaw, *J. Phys.: Condens. Matter* **1994**, *6*, 7499.
- [36] G. Kresse, J. Furthmüller, *Phys. Rev. B* **1996**, *54*, 11169.
- [37] J. Heyd, G. E. Scuseria, M. Ernzerhof, *J. Chem. Phys.* **2006**, *124*, 219906.
- [38] P. E. Blöchl, *Phys. Rev. B* **1994**, *50*, 17953.
- [39] G. Henkelman, B. Uberuaga, H. Jónsson, *J. Chem. Phys.* **2000**, *113*, 9901.
- [40] V. Gusakov, *J. Phys.: Condens. Matter* **2005**, *17*, S2285.
- [41] C. Freysoldt, B. Grabowski, T. Hickel, J. Neugebauer, G. Kresse, A. Janotti, C. G. Van de Walle, *Rev. Mod. Phys.* **2014**, *86*, 253.
- [42] E. Menéndez-Proupin, W. Orellana, *Phys. Status Solidi B* **2015**, *252*, 2649.
- [43] S. Lany, A. Zunger, *Phys. Rev. B* **2008**, *78*, 235104.
- [44] G. Mandel, *Phys. Rev.* **1964**, *134*, A1073.
- [45] M. A. Flores, W. Orellana, E. Menéndez-Proupin, *Phys. Rev. B* **2017**, *96*, 134115.
- [46] J. L. Roehl, S. V. Khare, *Sol. Energy Mater. Sol. Cells* **2014**, *128*, 343.
- [47] O. L. Maslyanchuk, L. A. Kosyachenko, S. V. Melnychuk, P. M. Fochuk, T. Aoki, *Phys. Status Solidi C* **2014**, *11*, 1519.